Arch. Metall. Mater. **71** (2026), 2, 583-586

DOI: https://doi.org/10.24425/amm.2026.158846

JIN KYU LEE[1*], SEONGHOON YI[2]

ENHANCED PLASTIC DEFORMATION BEHAVIOR OF $Zr_{62}Al_8Ni_{13}Cu_{17}$ BULK METALLIC GLASS MATRIX COMPOSITES REINFORCED WITH SIC PARTICLES

$Zr_{62}Al_8Ni_{13}Cu_{17}$ bulk metallic glass matrix composites reinforced with SiC particles were fabricated by spark plasma sintering using gas-atomized amorphous powders. The effects of SiC volume fraction on the microstructure and mechanical behavior were investigated. Dense microstructures with uniformly distributed SiC particles were obtained while preserving the amorphous matrix without crystallization. Compression tests demonstrated that the addition of SiC significantly enhanced both strength and plastic deformability. The composite containing 15 vol.% SiC exhibited a compressive strength of 1670 MPa and a total strain of 4.1%. The improved plasticity is attributed to the formation of multiple shear bands, suppression of shear band propagation, and enhanced interfacial stability associated with the viscous flow of the amorphous matrix.

Keywords: Bulk metallic glass; SiC; sintering; powder; viscous flow

1. Introduction

Bulk metallic glasses (BMGs) have attracted significant attention as advanced structural materials due to their exceptionally high strength and wide elastic limit compared to conventional crystalline metallic materials. Despite these advantageous properties, most BMGs exhibit extremely limited plastic deformability at room temperature. This behavior is primarily attributed to the highly localized concentration of shear stress during deformation, which results in the formation of a small number of dominant shear bands, leading to abrupt, catastrophic failure without appreciable plastic deformation [1-3]. To overcome this intrinsic brittleness, extensive efforts have been devoted to enhancing the plastic deformation capability of BMGs through the development of bulk metallic glass matrix composites. In this approach, a second phase is uniformly dispersed within the amorphous matrix to effectively hinder the localization of shear stress and suppress the uncontrolled propagation of individual shear bands. As a result, multiple shear bands can be activated throughout the material, promoting more homogeneous deformation and improved plasticity [4-5].

In recent years, powder metallurgy has emerged as a promising approach for fabricating bulk metallic glass matrix composites and tailoring their microstructural and mechanical properties [6-7]. The fabrication of composites by sintering mixtures of amorphous powders and second-phase powders offers considerable flexibility in material design, as the properties of the resulting composites can be readily adjusted by varying the type and volume fraction of the reinforcement phase. Moreover, when consolidation is conducted within the supercooled liquid region of the amorphous alloy, the Newtonian viscous flow behavior of the amorphous phase can be leveraged to enhance interfacial bonding between the amorphous matrix and the second phase, thereby improving the structural integrity of the composites [8-9].

In this study, Zr-based bulk metallic glass matrix composites (BMGMCs) reinforced with SiC as a secondary phase were fabricated using the spark plasma sintering process. The effects of SiC addition and its volume fraction on the microstructural evolution and plastic deformation behavior of the composites were systematically investigated.

2. Experimental

A master alloy with a nominal composition of $Zr_{62}Al_8Ni_{13}Cu_{17}$ (at.%) was prepared using a vacuum plasma melting system. The fabricated master alloy was then charged into the melting chamber of a vacuum gas atomization system and remelted at temperatures ranging from 1623 to 1723 K. Amorphous Zr-based powders were produced by gas atomization, and powders with particle

[1] KONGJU NATIONAL UNIVERSITY, DIVISION OF ADVANCED MATERIALS ENGINEERING, 1223-24, CHEONAN DAERO, SEOBUK-GU, CHEONAN-SI, CHUNGNAM, 31080, KOREA
[2] KYUNGPOOK NATIONAL UNIVERSITY, DAEGU, KOREA

* Corresponding author: jklee71@kongju.ac.kr

sizes below 90 μm were selected for subsequent experiments. Commercial SiC powders with a purity of 99% and particle sizes below 45 μm were used as the second-phase reinforcement. The amorphous Zr-based powders and SiC powders were mixed at volume ratios of 95:5, 90:10, and 85:15 using a ball milling system (Pulverisette 5, FRITSCH) operated at a rotational speed of 100 rpm for 30 minutes. The mixed powders were consolidated into bulk metallic glass matrix composites using spark plasma sintering (SPS). Before sintering, the powder mixtures were loaded into a tungsten carbide mold with a diameter of 13 mm and placed in the SPS chamber. The sintering process was carried out under a vacuum atmosphere of 5×10^{-2} Torr, with an applied uniaxial pressure of 600 MPa. The temperature was increased from room temperature to just below the crystallization temperature (T_x) of the amorphous alloy at a heating rate of 0.67 K/s.

The microstructures of the fabricated bulk metallic glass matrix composites were examined using optical microscopy (OM) and scanning electron microscopy (SEM, MIRA LMH, TESCAN). Phase identification was conducted by X-ray diffraction (XRD, MiniFlex600, Rigaku). The glass transition temperature (T_g), crystallization temperature, and crystallization enthalpy (ΔH) of the composites were determined by differential scanning calorimetry (DSC, DSC8000, PerkinElmer) over a temperature range of 373-873 K, with a heating rate of 0.67 K/s. Compressive mechanical properties were evaluated at room temperature using a universal testing machine (UTM, AG-X, SHIMADZU) at a strain rate of 1×10^{-4} s^{-1}. After the compression tests, the fracture surfaces of the specimens were examined using SEM.

3. Results and discussion

Fig. 1(a)-(c) shows the microstructures of $Zr_{62}Al_8Ni_{13}Cu_{17}$ BMGMCs containing 5, 10, and 15 vol.% SiC, fabricated by the SPS process. In all compositions, the SiC particles, acting as the secondary phase, are uniformly distributed within the amorphous $Zr_{62}Al_8Ni_{13}Cu_{17}$ matrix. Furthermore, a dense and defect-free microstructure – without observable pores or interfacial debonding – is formed at the matrix-reinforcement interfaces. This well-consolidated microstructure is attributed to the viscous flow behavior of the amorphous powders within the supercooled liquid region during SPS, which facilitates effective densification and strong interfacial bonding [10-11]. Furthermore, the SiC particles predominantly retain their original angular morphology, indicating that no significant morphological changes or interfacial reactions occurred during the sintering process. The preservation of morphology suggests that the mechanical properties of BMGMCs are largely retained, as the size, distribution, intrinsic properties, and volume fraction of the second-phase particles primarily determine these properties. When the second phase is uniformly dispersed within the amorphous matrix, it can serve as nucleation sites for shear band initiation while simultaneously impeding shear band propagation, thereby reducing strain localization [12]. Fig. 1(d) presents the XRD patterns of the gas-atomized Zr-based amorphous powders and the Zr-based BMGMCs fabricated by SPS. The XRD pattern of the Zr-based amorphous powders exhibits only a broad halo peak characteristic of an amorphous structure, with no detectable diffraction peaks corresponding to crystalline phases, confirming the formation of a fully amorphous phase. In contrast, the XRD patterns of the BMGMCs display a superposition of the amorphous halo from the Zr-based metallic glass matrix and distinct diffraction peaks corresponding to crystalline SiC. These results clearly indicate the successful fabrication of BMGMCs consisting of an amorphous matrix reinforced with SiC. Notably, no additional crystalline peaks other than those of SiC were observed, demonstrating that crystallization of the amorphous matrix was effectively suppressed during the SPS process.

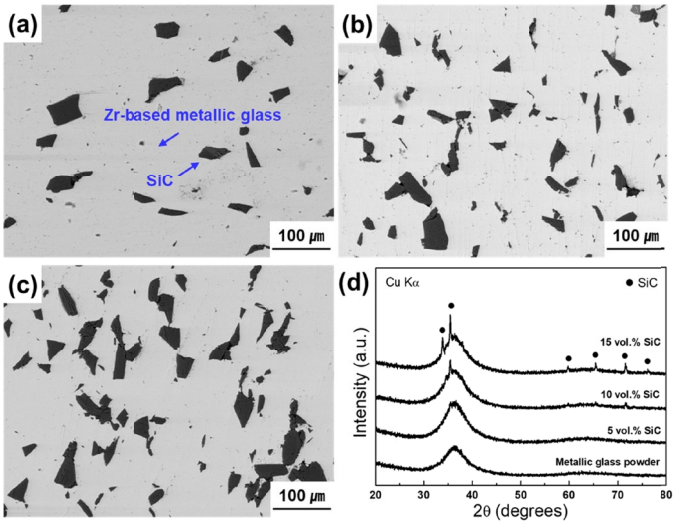

Fig. 1. SEM micrographs of $Zr_{62}Al_8Ni_{13}Cu_{17}$ BMG composites with SiC contents of (a) 5, (b) 10, and (c) 15 vol.%; (d) XRD patterns of the metallic glass powder and the corresponding composites

Fig. 2 presents the DSC results of the fabricated BMGMCs, obtained at a heating rate of 0.67 K/s. The DSC curves display an endothermic event corresponding to the glass transition, followed by a single exothermic peak associated with crystallization. The

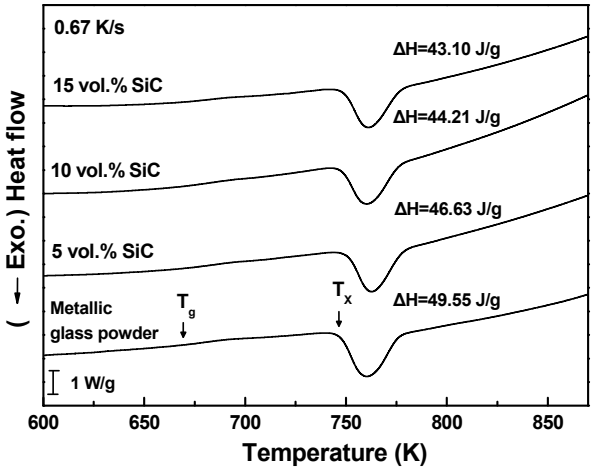

Fig. 2. DSC curves obtained from the $Zr_{62}Al_8Ni_{13}Cu_{17}$ metallic glass powder and $Zr_{62}Al_8Ni_{13}Cu_{17}$ BMG composites containing SiC phase

glass transition temperature (T_g) and crystallization temperature (T_x) of the amorphous composites containing the SiC phase are comparable to those of the Zr-based amorphous alloy powders, indicating similar thermal behavior. Compression tests were conducted to evaluate the mechanical properties of the fabricated Zr-based composites, with a particular focus on the effect of the SiC phase on BMGMCs.

Fig. 3 presents the compressive stress-strain curves of the Zr-based BMG and BMGMCs obtained after spark plasma sintering. The monolithic Zr-based BMG exhibits a compressive strength of approximately 1580 MPa and undergoes catastrophic failure without any observable plastic deformation. In contrast, the BMGMC containing 15 vol.% SiC shows a maximum compressive strength of 1670 MPa, a total compressive strain of 4.1%, and a plastic strain of 2.1%. To investigate the role of the SiC phase in the post-yield plastic deformation behavior of Zr-based BMGMCs, compression loading was applied to the BMGMC specimens and subsequently unloaded just before fracture after yielding. The shear bands formed on the specimen surface were then examined. Fig. 4 presents the surface microstructure of the $Zr_{62}Al_8Ni_{13}Cu_{17}$ BMGMC containing 15 vol.% SiC, where multiple shear bands are observed to initiate at the interfaces between the amorphous matrix and the SiC phase. In some regions, intersections between primary and secondary shear bands are also observed. It has been reported that in amorphous matrix composites containing a second phase, the application of compressive loading induces heterogeneous strain and stress fields due to the elastic and plastic property mismatch between the amorphous matrix and the reinforcement phase, leading to localized stress concentration regions that serve as preferred sites for shear band initiation [5,13]. Accordingly, in the present Zr-based BMGMCs, stress concentration is expected to develop at the interfaces between the amorphous matrix and the SiC particles, thereby promoting the nucleation of shear bands in these regions. As the shear bands propagate through the amorphous matrix, their advance is impeded upon encountering additional SiC particles or intersecting with other shear bands, effectively suppressing catastrophic shear localization and contributing to the enhanced plastic deformation behavior

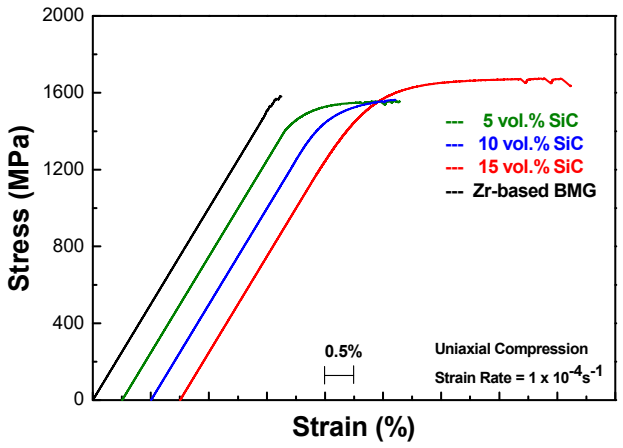

Fig. 3. Compressive stress-strain curves of $Zr_{62}Al_8Ni_{13}Cu_{17}$ BMG and $Zr_{62}Al_8Ni_{13}Cu_{17}$ BMG composites containing SiC phase

of the composites. In BMGMCs, the formation of multiple shear bands facilitates interactions among shear bands. Meanwhile, the presence of primary shear bands together with the heterogeneous stress distribution induced by second-phase particles is known to impede the propagation of secondary shear bands formed along planes of maximum shear stress [14]. These second-phase particles act as effective barriers to the propagation of dominant shear bands, thereby suppressing the rapid propagation of shear bands and preventing premature failure [15].

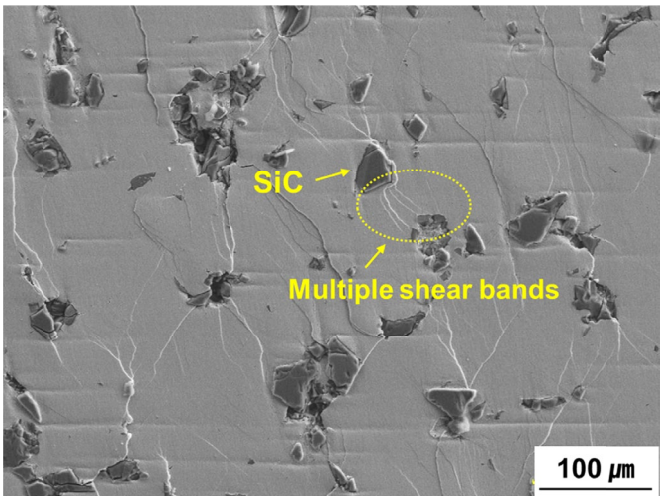

Fig. 4. SEM micrographs obtained from the surface of $Zr_{62}Al_8Ni_{13}Cu_{17}$ BMG composites containing 15 vol.% SiC phase just before fracture.

Accordingly, Zr-based BMGMCs with enhanced plastic deformability were successfully fabricated by mixing gas-atomized $Zr_{62}Al_8Ni_{13}Cu_{17}$ amorphous powders with SiC powders, followed by spark plasma sintering. The observed improvement in plastic strain can be attributed to the combined effects of multiple shear band formation and the effective suppression of shear band propagation arising from interactions with the SiC second phase.

4. Conclusions

In this study, we fabricated BMGMCs by mixing gas-atomized $Zr_{62}Al_8Ni_{13}Cu_{17}$ amorphous powders with SiC powders, then consolidated the mixture using spark plasma sintering. We systematically investigated the effect of the SiC second-phase volume fraction on plastic deformation behavior. A $Zr_{62}Al_8Ni_{13}Cu_{17}$ amorphous composite containing 15 vol.% SiC exhibited a compressive strength of 1670 MPa and a total strain of 4.1%. The enhanced plastic deformation arises from the uniformly distributed SiC particles within the amorphous matrix. These particles not only initiate shear band formation but also impede the propagation of shear bands, promoting stress redistribution and enabling plastic deformation over a wider strain range. Improved plastic deformability is also linked to excellent interfacial stability, which results from viscous flow-assisted superplastic deformation of the amorphous phase within the supercooled liquid region.

Acknowledgments

This work was supported by the research grant of Kongju National University Industry-University Cooperation Foundation in 2024

REFERENCES

[1] A.S. Argon, Plastic deformation in metallic glasses. Acta Metall. **27** (1), 47-58 (1979).
DOI: https://doi.org/10.1016/0001-6160(79)90055-5

[2] A.L. Greer, Y.Q. Cheng, E. Ma, Shear bands in metallic glasses. Mater. Sci. Eng. R **74** (4), 71-132 (2013).
DOI: https://doi.org/10.1016/j.mser.2013.04.001

[3] J.J. Lewandowski, A.L. Greer, Temperature rise at shear bands in metallic glasses. Nat. Mater. **5**, 15-18 (2006).
DOI: https://doi.org/10.1038/nmat1536

[4] C.C. Hays, C.P. Kim, W.L. Johnson, Microstructure controlled shear band pattern formation and enhanced plasticity of bulk metallic glasses containing in situ formed ductile phase dendrite dispersions. Phys. Rev. Lett. **84**, 2901-2904 (2000).
DOI: https://doi.org/10.1103/PhysRevLett.84.2901

[5] D.C. Hofmann, J.Y. Suh, A. Wiest, G. Duan, M.L. Lind, W.L. Johnson, Designing metallic glass matrix composites with high toughness and tensile ductility. Nature **451**, 1085-1089 (2008).
DOI: https://doi.org/10.1038/nature06598

[6] G.Q. Xie, D.V. Louzguine-Luzgin, A. Inoue, Characterization of interface between the particles in NiNbZrTiPt metallic glassy matrix composite containing SiC fabricated by spark plasma sintering. J. Alloys Compd. **483**, 239-242 (2009).
DOI: https://doi.org/10.1016/j.jallcom.2008.07.226

[7] S. Zhu, G. Xie, F. Qin, X. Wang, T. Hanawa, Ti particles dispersed Ti-based metallic glass matrix composite prepared by spark plasma sintering. Mater. Trans. **53 (8)**, 1335-1338 (2013).
DOI: https://doi.org/10.2320/matertrans.MF201311

[8] G.Q. Xie, D.V. Louzguine-Luzgin, H. Kimura, A. Inoue, F. Wakai, Large-size ultrahigh strength Ni-based bulk metallic glassy matrix composites with enhanced ductility fabricated by spark plasma sintering. Appl. Phys. Lett. **92**, 121907 (2008).
DOI: https://doi.org/10.1063/1.2902282

[9] G.Q. Xie, D.V. Louzguine-Luzgin, F. Wakai, H. Kimura, A. Inoue, Microstructure and properties of ceramic particulate reinforced metallic glassy matrix composites fabricated by spark plasma sintering. Mater. Sci. Eng. B **148**, 77-81 (2008).
DOI: https://doi.org/10.1016/j.mseb.2007.09.027

[10] J.K. Lee, H.J. Kim, T.S. Kim, S.Y. Shin, Y.C. Kim, J.C. Bae, Deformation behavior of Ni-based bulk metallic glass synthesized by spark plasma sintering. J. Mater. Process. Technol. **187-188** (12), 801-804 (2007).
DOI: https://doi.org/10.1016/j.jmatprotec.2006.11.206

[11] J.K. Lee, J.P. Lee, Synthesis of Al-Ni-Co-Y Bulk Metallic Glass fabricated by Spark Plasma Sintering. J. Powder Mater. **30** (1), 41-46 (2023).
DOI: https://doi.org/10.4150/kpmi.2023.30.1.41

[12] F. Abdeljawad, M. Fontus, M. Haataja, Ductility of bulk metallic glass composites: Microstructural effects. Appl. Phys. Lett. **98** (3), 031909 (2011).
DOI: https://doi.org/10.1063/1.3531660

[13] P. Gargarella, S. Pauly, K.K. Song, J. Hu, N.S. Barekar, M. Samadi Khoshkhoo, A. Teresiak, H. Wendrock, U. Kühn, C. Ruffing, E. Kerscher, J. Eckert, Ti–Cu–Ni shape memory bulk metallic glass composites. Acta Mater. **61** (1), 151-162 (2013).
DOI: https://doi.org/10.1016/j.actamat.2012.09.042

[14] S. Scudino, B. Jerliu, S. Pauly, K.B. Surreddi, U. Kühn, J. Eckert, Ductile bulk metallic glasses produced through designed heterogeneities. Scripta Mater. **65** (9), 815-818 (2011).
DOI: https://doi.org/10.1016/j.scriptamat.2011.07.039

[15] K. Geng, W. Yang, J. Mo, H. Liu, F. Wei, Z. Ma, Y. Zhao, A. Inoue, Plastic deformation mechanism of ductile $Fe_{50}Ni_{30}P_{13}C_7$ metallic glass. Met. Mater. Int. **25**, 487-498 (2019).
DOI: https://doi.org/10.1007/s12540-018-0181-9